Published in final edited form as:

ACS Chem Biol. 2021 November 19; 16(11): 2244–2254. doi:10.1021/acschembio.1c00379.

Spontaneous cleavage at Glu and Gln residues in long-lived proteins

Michael G. Friedrich[1],

Zhen Wang[2],

Kevin L. Schey[2],

Roger J. W. Truscott[1]

[1]Illawarra Health and Medical Research Institute, University of Wollongong, Wollongong, NSW, 2522, Australia

[2]Department of Biochemistry and Mass Spectrometry Research Center, Vanderbilt University School of Medicine, Nashville, TN, USA

Abstract

Long-lived proteins (LLPs) are prone to deterioration with time and one prominent breakdown process is scission of peptide bonds. These cleavages can either be enzymatic or spontaneous. In this study, human lens proteins were examined and many were found to have been cleaved on the C-terminal side of Glu and Gln residues. Such cleavages could be reproduced experimentally by *in vitro* incubation of Glu- or Gln-containing peptides at physiological pHs. Spontaneous cleavage was dependent on pH and amino acid sequence. These model peptide studies suggested that the mechanism involves a cyclic intermediate and is therefore analogous to that characterised for cleavage of peptide bonds adjacent to Asp and Asn residues. An increased amount of some Glu/Gln cleaved peptides in the insoluble fraction of human lenses suggests that cleavage may act to destabilise proteins. Spontaneous cleavage at Glu and Gln, as well as recently described crosslinking at these residues, can therefore be added to the similar processes affecting long-lived proteins that have already been documented for Asn and Asp residues.

Keywords

Protein Cleavage; Human lens; Huntington’s disease; Long-lived proteins; Age

Introduction

Throughout the body, cells that are life-long or long-lived are more common than previously thought [1–3]. From brain to testis, many cells have been discovered to have a long lifespan. [4] Within these cells, a number of LLPs have been found [5]. The lifetimes of these proteins lead to an array of modifications; both enzymatic and spontaneous. Post-translation modifications (PTMs) such as oxidation [6], glycation [7], acylation [8], citrullination [9],

Funding sources and disclosure of conflicts of interest Funding for this study was provided by National Institutes of Health by grants R01 EY024258 and P30 EY008126. The authors declare no conflict of interest.

deamidation [10], isomerisation [11], racemisation [12, 13] and others have been reported in aged tissues [14]. Some enzymatic modifications have been well-established however mechanisms of spontaneous deterioration are currently not well understood. In the human lens, such processes are likely to be responsible for the formation of cataract and this has been reviewed recently [15, 16].

The lens is an ideal tissue to investigate spontaneous processes that occur to LLPs because the center, or nucleus, of the adult human lens does not contain active enzymes [17, 18]. This is due to the unique growth pattern of the lens [19] whereby during fiber cell maturation organelles are degraded resulting in central lens proteins that are as old as the organism.[20] Current knowledge suggests that five spontaneous processes are prevalent in LLPs during aging: racemisation [13], isomerisation [11, 12], deamidation [10], crosslinking [21–23] and peptide bond cleavage [24]. Under normal physiological conditions, most peptide bonds are stable [25], however spontaneous scission of some peptide bonds, such as those adjacent to Asn, Asp, Ser, Thr, Cys residues have been reported [24, 26, 27]. In some cases, other factors, such as transition metals, can influence these spontaneous cleavage reactions. For example, zinc can catalyse cleavage of peptide bonds on the N-terminal side of Ser and Thr residues [24].

Cleavage of peptide bonds next to Asp has been known to peptide chemists for many years [28]. The mechanism of Asp cleavage appears to involve attack of the ionized carboxyl side chain on the protonated carbonyl group of the peptide bond [29]. In the case of Asn cleavage, the side chain nitrogen atom attacks the carbonyl of the adjacent peptide bond [30]. Such reactions lead to cleavage of lens proteins next to Asp and Asn residues in lens proteins [30, 31]

As part of an ongoing project to determine the main spontaneous processes that occur to LLPs, proteomic techniques were employed to analyse protein modifications in adult human lenses. In this paper, evidence was found for the scission of peptide bonds on the C-terminal side of Gln and Glu residues. Further, the mechanism of spontaneous cleavage was investigated by the use of model peptides.

Results and Discussion

Identification of Gln and Glu cleavage sites in human lenses

Previously it has been reported that LLPs are susceptible to spontaneous cleavage at Asp and Asn residues and that this is mediated via a 5-membered cyclic intermediate [30, 31]. In a similar manner, both Gln and Glu can undergo an intramolecular reaction forming a six-membered cyclic intermediate. To investigate whether this process could cause protein cleavage in biological tissues, we investigated tryptic peptides from human lens proteins for evidence of non-tryptic polypeptide cleavage at Gln and Glu residues. A diverse set of proteins including cytosolic, cytoskeletal and membrane proteins were found to display evidence of cleavage at Gln (Table 1) and Glu (Table 2).

Quantification Glu and Gln truncation

Based on MaxQuant search results and overall peptide intensities, six truncation sites were selected for quantification studies. These six sites include E165 and E156 in αA-crystallin, Q208 in βA3-crystallin, Q189 in βA4-crystallin, E249 in βB1-crystallin and Q197 in βB2-crystallin. Manual verification was performed for these truncated peptides based on accurate mass, retention time, isotopic distribution and tandem mass spectra. Once verified as *bona fide* truncation products, peak intensities were obtained using the Xcalibur ICIS peak integration algorithm. Peak areas of the truncated peptides were normalized by peak areas of the corresponding tryptic peptide. The levels of truncation were compared between different solubility fractions and lens regions. The results can be found in Figure 1. Since the tryptic peptides used for normalization have different ionization efficiencies, the y-axis in Figure 1 simply provides a measure of the relative degree of truncation.

Relative truncation at E165 and E156 of αA, Q208 of βA3, and Q189 of βA4 increased in the USF or UIF compared to WSF, indicating truncation at these sites may induce protein insolubilisation. Increased truncation at αA E156, βA3 Q208 in USF and UIF samples was detected in all three regions of the lens (cortex, outer nucleus and inner nucleus). Truncation levels in USF and UIF were also compared and no statistically significant difference was detected for these six truncation sites. Increased truncation in USF was not detected for all crystallin truncation sites. Truncation at E249 of βB1 and Q197 of βB2 in WSF and USF or UIF did not show a significant difference in any lens region.

The above truncation sites at Gln or Glu residues are close to the C-terminus of each protein. Significant levels of truncation can be detected in the cortex region. Only truncation at αA E165 and βA4 Q189 increased significantly in the inner nucleus region in USF compared with cortex region.

Common sites of cleavage

From Tables 1 & 2 it is apparent that cleavage on the C-terminal side of Gln and Glu residues is common, with 38 sites found cleaved next to Gln and 51 next to Glu. To understand the mechanism for the cleavage, model studies were undertaken using synthetic peptides. Two sets of peptides Ac-FAEXA and Ac-FAQXA were examined, where X corresponds to a Pro, Ala or Asp residue. These three amino acid residues were represented at protein cleavage sites for both Glu and Gln (see Supp Fig 3). The α-amino group was blocked by acetylation to avoid unwanted reactions during long incubation times. While fragments arising next to C-terminal Ser residues were common sites from the lens protein data, this residue was excluded from the peptide study since scission of the peptide bond N-terminal to a Ser can occur via other spontaneous mechanisms independent of Glu or Gln [37].

Cleavage at Glu residues

C-terminal Proline residue—To determine if spontaneous cleavage could be detected using model peptides, Ac-FAEPA was incubated in 50 mM sodium acetate buffer, pH 4.0 and the breakdown of Ac-FAEPA monitored by HPLC (Figure 2). After several days of incubation at 60°C, a peak eluting at 19.7 min was formed. Upon isolation and subsequent

analysis by mass spectrometry, it was found to contain Ac-FAE (Figure 3). The identity of this C-terminal Glu cleavage product was confirmed by co-elution and the MS/MS spectrum of synthetic Ac-FAE. While not visible in the HPLC trace, the dipeptide PA was also detected in the void volume and its identity was confirmed by mass spectrometry. After 25 days ~13% of the original Ac-FAEPA peptide had been cleaved.

The effect of pH on peptide bond scission was then examined using buffers more typical of physiological pHs, i.e. pH 6.7, 7.0 and 7.4 (Figures 2 and 4). Overall, the apparent rate of cleavage decreased considerably as buffer pH was increased. The rates were similar at pH 7.0 and at the pH of the centre of the lens (pH 6.7), however, the rate was significantly lower at pH 7.4. By comparison with pH 4.0, it was estimated that cleavage was approximately 18-fold slower at pH 6.7.

The above experiments were repeated at 37°C. While not visible by HPLC, Ac-FAE was detectable by mass spectrometry in the pH 4.0 and 6.7 incubations after 40 days. No evidence of Ac-FAE was found in the pH 7.0 and 7.4 incubations.

C-terminal Aspartate residue—Using the same incubation conditions as Ac-FAEPA, the HPLC profile of Ac-FAEDA after 25 days incubation at pH 4.0 was more complex than that of Ac-FAEPA. This is presumably due to the presence of an Asp residue in the sequence, since spontaneous cleavage next to Asp has been documented [31] and L-Asp residues can also convert to D-Asp as well as to D- isoAsp and L- isoAsp via a succinimide (Asu) intermediate [38].

Two early eluting HPLC peaks were found to be cleavage products of Ac-FAEDA. A peak eluting at 77 min was confirmed by mass spectrometry to be Ac-FAE. A second peak at 79 min was identified by MS/MS as the Asp cleavage product Ac-FAED, which is consistent with previous studies showing cleavage at Asp [31]. Cleavage at both Glu and Asp decreased as buffer pH was increased, and at pH 7.4 little cleavage was observed (Figure 4). A peak at approximately 86 min was shown by mass spectrometry to have the same mass as Ac-FAEDA and is likely due to the formation of Ac-FAE(isoAsp)A. Detection of a component corresponding in mass and MS/MS to Ac-FAE(Asu)A at 98 min supported this assignment.

Similar to the previous incubation of Ac-FAEPA, when Ac-FAEDA was incubated at 37°C for 40 days, Ac-FAE was detected by mass spectrometry in both the pH 4.0 and 6.7 samples.

C-terminal Alanine residue—In contrast to Ac-FAEPA and Ac-FAEDA, Ac-FAEAA showed considerably less spontaneous cleavage next to Glu (Figure 4). At pH 4.0, little cleavage was observed in the case of Ac-FAEAA and this decreased at higher pHs, with none detected at pH 7.4.

Cleavage at Gln residues

The above experiments were repeated using the homologous Gln peptides.

C-terminal Proline residue—Unlike the case of Ac-FAEPA, where the formation of Ac-FAE was readily observed, Ac-FAQPA displayed little breakdown even after 25 days incubation at pH 4.0 (Figure 5a). A small peak was observed by HPLC following 25 days of incubation and was confirmed by mass spectrometry and the use of synthetic standards to be Ac-FAQ (Figure 3b). No Ac-FAQ was detected in incubations at pH 6.7, 7.0 and 7.4 after 25 days.

C-terminal Aspartate residue—By contrast to Ac-FAQPA, the HPLC traces of Ac-FAQDA incubations displayed multiple breakdown products. At pH 4.0, the two major products generated were Ac-FAQ and Ac-FAQD and there was no evidence of deamidation of Gln occurring or the generation of Ac-FAE (Supplemental Figure 2). Each product was identified by mass spectrometry.

At pH 6.7, Ac-FAQ was detected in low amounts, together with the major breakdown products resulting from isomerisation and cleavage at Asp i.e. the formation of Ac-FAQ(isoAsp)A and Ac-FAQD. As the pH of incubation increased from 7.0 to 7.4, the amount of Ac-FAQ formed decreased (Figure 5b).

C-terminal Alanine residue—For Ac-FAQAA, cleavage was very pH dependent (Figure 5). At pH 4.0 no cleavage was observed, however as the pH rose to 6.7, Ac-FAQ was detected but the rate of formation decreased thereafter as pH increased to 7 and 7.4. By comparison with Ac-FAEAA, cleavage of Ac-FAQAA occurred 3-fold and 2.5-fold faster at pH 6.7 and 7.0 respectively.

N-terminal Cleavage at Glu—In addition to Ac-FAE production from the Glu peptide incubations described above, other peptide samples displayed evidence of N-terminal cleavage that was detectable via mass spectrometry. In samples of Ac-FAEPA and Ac-FAEDA that had been incubated at pH 4.0 and 6.7, EPA and EDA were found. In addition, the N-terminal fragment, Ac-FA, was also detected, although these cleavage products were present only in trace amounts. No similar cleavages were observed in the case of the Gln containing peptides.

Discussion

This study has shown that Glu and Gln residues can act as sites for spontaneous cleavage in LLPs. Further, truncation at Glu or Gln was more pronounced in some crystallins in the insoluble protein fractions (figure. 1) suggesting that truncation at Glu or Gln could induce protein insolubilization. In this paper, a mechanism by which the side chains of these residues can function to cleave adjacent peptide bonds is proposed.

In general, cleavage observed at Glu and Gln was dependent on pH and was slower than that observed at Asp/Asn. At approximately neutral pH, cleavage at Glu was comparable to Gln, however Glu cleavage displayed a marked decline in going from the pH in the lens center (pH 6.7) to pH of blood (pH 7.4). At acidic pH, cleavage occurred more readily at Glu. To illustrate this point, at the pH of lysozomes (pH 4.0) no spontaneous cleavage next to Gln

was detected in Ac-FAQAA in comparison to Ac-FAEAA. Cleavage was also dependent on the nature of the amino acid C-terminal to the Glu or Gln as illustrated in Supp Fig 3

Data from human lenses revealed numerous sites of peptide bond scission at Gln and Glu resides and these cleavages were predominantly localised on the C-terminal side of these amino acids. Such reactions could be replicated using peptides, demonstrating that the reactions can occur spontaneously. Although not investigated in detail, the mechanism seems to involve the formation of a cyclic intermediate, as found with the homologous Asp and Asn residues [30, 31]. In the case of Gln and Glu residues, cyclisation results in either the formation of a C-terminal glutarimide (GSU) or a glutaric anhydride respectively. Hydrolysis of these intermediates leads to scission of the peptide bond.

It is hypothesised that cleavage at Gln residues occurs when the peptide backbone carbonyl group is attacked by the nitrogen atom of the side chain amide (Figure 6). The formation of a GSU ring has been shown to be important in the deamidation of glutamine residues [39]. In addition, identification of isoGlu residues confirmed the involvement of GSU in studies of glutamine deamidation [40]. Hydrolysis of the resulting cyclic GSU yields a C-terminal Gln residue. Similarly, with Glu residues, the side chain carboxyl oxygen atom attacks the peptide backbone carbonyl group resulting in the formation of a cyclic anhydride. It was apparent from the model studies, that the rates of peptide bond scission at Gln/Glu residues are significantly lower than those found with Asp and Asn. This was clearly seen in the peptides that contained Asp as well as Glu/Gln, such as Ac-FAEDA and Ac-FAQDA, where cleavage at Asp was more prominent than that at Glu or Gln.

In addition to C-terminal cleavage at Glu residues, cleavage was detected N-terminally to Glu in model peptides. This was not observed in peptides containing Gln, nor was it observed in tryptic peptides from the human lens samples. Interestingly cleavage N-terminal to Glu can be facilitated by bromination of the Glu side chain, encouraging the formation of a five -membered ring [41].

In previous studies it was found that long-lived lens proteins are cleaved and that the amount of hydrolysis increases with age [42]. In these endogenous peptides, some residues such as Ser occur more commonly on the N-termini and this was explained by a spontaneous process of peptide bond hydrolysis in lens crystallins. In the case of Ser, cleavage of the N-terminal peptide bond was facilitated by zinc [24]. When these same data were examined for the frequency of Glu and Gln termini, Gln residues occurred more frequently on the C-terminal side, however this was not the case for Glu. Recently we discovered that Glu and Gln can act as sites of covalent crosslinking [43]. In these cases, sites of crosslinking within intermediate filament proteins such as phakinin and filensin were relatively more abundant than in crystallins, for reasons that are at present unknown. While not examined in this study, if cleavage at Gln or Glu occurred via a cyclic glutarimide or glutaric anhydride a potential crosslink could form analogous to what has been observed at Asn and Asp [30, 31]. Evidence of a C-terminal Glu crosslink occurring in peptide models has been previously reported [43].

In this study only lens proteins were examined. Proteins within other tissues may also show evidence of spontaneous cleavage at Glu or Gln, such as polypeptides containing large polyQ tracts. For example, known polyglutamine disorders (Huntingtons disease [44], spinal and bulbar muscular atrophy [44], dentatorubro-pallidolysian atrophy [44], spinocerebellar ataxias [44],) are characterised by expanded polyQ sequences within their respective disease-causing proteins. Little is known about cleavages within these polyQ regions and this will be investigated in the next phase of this research.

In conclusion, this study has revealed that cleavage next to Gln and Glu occurs in a diverse set of proteins in the human lens. Recently we discovered that Glu and Gln residues can also act as sites of novel covalent crosslinking [43]. There are therefore parallels between the Asp/Asn pair and the homologous Glu/Gln amino acids, in terms of their propensity to act as sites for spontaneous crosslinking, as well as sites of cleavage, in long-lived proteins.

Methods:

Lens protein extraction

Frozen human lenses were obtained from NDRI (Philadelphia, PA). All lenses were isolated from donors no later than 8 hours post mortem and shipped on dry ice. Human lens work was conducted in compliance with the Declaration of Helsinki. All lenses received were stored at −80°C until use. Four normal human lenses were used (48 yr, 56 yr and two 53 yr).

Lenses were individually dissected into three regions: cortex, outer nucleus and inner nucleus. As the lens grows continuously throughout life with no turnover of protein, the centre of the lens corresponds to the oldest crystallins, the outer nucleus is of intermediate age and the cortex contains the youngest crystallins [32].

Samples corresponding to different regions of the lenses and different solubilities were prepared as described previously [33]. Briefly, human lenses were equatorially sectioned to a thickness of 30 μm in a cryostat (LEICA CM 3050S, Leica Microsystems Inc., Bannockburn, IL) and sections were collected on pieces of parafilm. Three different regions of the lens were separated by sequentially punching the sections using AcuPunch trephines (Acuderm Inc, Ft. Lauderdale, FL) with diameters of 4.5 mm, 6 mm to generate the inner nucleus and the outer nucleus regions. The rest of the tissue was collected as the cortex. Lens sections on parafilm rings were prepared by five sequential washes with 100 μL of 25 mM Tris, 150 mM NaCl, 5 mM EDTA, pH 7.4. The samples were passed through a 25G needle five times and centrifuged at 20,000 g for 30 min. The supernatant was collected as the water soluble fraction (WSF). The pellets were vortexed in 100 μL of 8 M urea in 25 mM Tris, 150 mM NaCl, 5 mM EDTA, pH 7.4 and centrifuged at 20,000g for 30 min. This 8M urea extraction was repeated and both urea extracts were pooled as the urea soluble fraction (USF). The remaining pellets were collected as the urea insoluble fraction (UIF). The protein concentration in each fraction was measured by BCA assay (Thermo Scientific, Rockford, IL). Samples were reduced and alkylated as described previously [33]. WSF and USF proteins were precipitated by chloroform/methanol as previously described [34]. All samples were digested by trypsin in 50mM Tris containing 10% acetonitrile, pH 8.0 with an enzyme-to-protein ratio of 1:100. The digestion was done overnight at 37°C. After digestion,

all samples were dried in a speedvac and peptides in each sample were reconstituted in 0.1% formic acid for further analysis.

LC-MS/MS

For LC-MS/MS analysis, tryptic peptides were separated on a one-dimensional fused silica capillary column (250 mm × 100 μm) packed with Phenomenex Jupiter resin (3 μm, 300 Å pore size) coupled with an Easy-nLC system (Thermo Scientific, San Jose, CA). A 70-minute gradient was performed, consisting of the following: 0–60 min, 2–45% ACN (0.1% formic acid); 60–70 min, 45–95% ACN (0.1% formic acid) balanced with 0.1% formic acid. The eluate was directly infused into a Q Exactive instrument (Thermo Scientific, San Jose, CA) equipped with a nanoelectrospray ionization source. The data-dependent instrument method consisted of MS1 acquisition (R=70,000), using an MS AGC target value of 1e6, followed by up to 15 MS/MS scans (R=17,500) of the most abundant ions detected in the preceding MS scan. The MS2 AGC target value was set to 2e5, with a maximum ion time of 200 ms, and a 5% underfill ratio, and an intensity threshold of 5e4. HCD collision energy was set to 27, dynamic exclusion was set to 5 s, and peptide match and isotope exclusion were enabled.

Incubation of Glu and Gln peptides

Peptides Ac-FAEDA, Ac-FAEPA, Ac-FAEAA, Ac-FAQDA, Ac-FAQPA and Ac-FAQAA (1 mg/mL) were incubated at either 37 °C or 60 °C in 50mM MOPS buffer at pH 6.7, 7.0 and 7.4 or 50mM sodium acetate buffer at pH 4.0. Aliquots were collected at various time intervals and were injected onto an Agilent 1100 HPLC using an Aeris RP-HPLC column (2.6 μ, XB-C18, 100 × 2.1 mm, Phenomenex). Breakdown products of peptides Ac-FAQDA and Ac-FAEDA were eluted with the following gradient 2% ACN, 0.1% TFA 0–40 min, 5% ACN, 0.1% TFA 40–60 mins, 10% ACN, 0.1%TFA 60–80 min, 15% ACN, 0.1% TFA 80–100min, 25% ACN, 0.1% TFA 100–120 min, 80 % ACN, 0.1%TFA, 135 min 2% ACN, 0.1%TFA 145min. All other peptides used the following elution gradient: 2% ACN, 0.1% TFA 5 min, 20% ACN, 0.1% TFA 15 mins, 40% ACN, 0.1%TFA 20 min, 25 min 80%ACN, 0.1% TFA, 35 min 80% ACN, 0.1% TFA, 30.1 min 2% ACN, 0.1%TFA, 40 min 2% ACN, 0.1%TFA.

Breakdown of all peptides was monitored at 216nm and 280nm. Peaks were collected and identified by tandem mass spectrometry on an LTQ Orbitrap Fusion Tribrid with a nanoelectrospray ionisation source (Thermo Scientific, San Jose, CA). Data were manually acquired with HCD collision energy set to 15.

Data analysis

For identifying sites of truncation, the raw data were loaded into MaxQuant software (http://maxquant.org/, version 1.6.6.0) [35] and searched against a custom human lens database [36]. The search was performed with semi-tryptic specificity with a maximum of 2 missed cleavage sites. Methionine oxidation, asparagine deamidation and protein N-terminal acetylation were variable modifications (up to 2 modifications allowed per peptide); cysteine was assigned a fixed carbamidomethyl modification. Precursor mass tolerance was set at 5 ppm. A false discovery rate (FDR) of 1% was applied for both peptide and protein

filtering. To quantify the levels of truncation, selected ion chromatograms were generated for truncated peptides and peak areas were calculated within Xcalibur software 4.0.27.19 (ThermoFisher Scientific, San Jose, CA). The peak areas of the truncated peptides were normalized by the peak intensities of corresponding tryptic peptides. The peak areas of the tryptic peptides were obtained from MaxQuant search result. Statistical analysis was performed by Student's t-test and results were considered as statistically significant when $p<0.05$.

Supplementary Material

Refer to Web version on PubMed Central for supplementary material.

Acknowledgements:

The authors acknowledge the use of the UOW Mass Spectrometry User Resource and Research Facility (MSURRF), University of Wollongong and the Proteomics Core Facility of the Vanderbilt University Mass Spectrometry Research Center.

References

1. Fornasiero EF, et al. , Precisely measured protein lifetimes in the mouse brain reveal differences across tissues and subcellular fractions. Nature Communications, 2018. 9(1): p. 4230.
2. Toyama BH, et al. , Visualization of long-lived proteins reveals age mosaicism within nuclei of postmitotic cells. J Cell Biol, 2019. 218(2): p. 433–444. [PubMed: 30552100]
3. Truscott RJW, Schey KL, and Friedrich MG, Old Proteins in Man: A Field in its Infancy. Trends in biochemical sciences, 2016. 41(8): p. 654–664. [PubMed: 27426990]
4. Truscott RJW, Long-Lived Cells and Long-Lived Proteins in the Human Body, in Long-lived Proteins in Human Aging and Disease. 2021. p. 5–42.
5. Toyama BH and Hetzer MW, Protein homeostasis: live long, won't prosper. Nature Reviews Molecular Cell Biology, 2013. 14(1): p. 55–61. [PubMed: 23258296]
6. Gorisse L, et al. , Protein carbamylation is a hallmark of aging. Proceedings of the National Academy of Sciences, 2016. 113(5): p. 1191.
7. Sivan SS, et al. , Age-related accumulation of pentosidine in aggrecan and collagen from normal and degenerate human intervertebral discs. The Biochemical journal, 2006. 399(1): p. 29–35. [PubMed: 16787390]
8. Lu J-Y, et al. , Protein acetylation and aging. Aging, 2011. 3(10): p. 911–912. [PubMed: 22067362]
9. Kim JK, et al. , Multiple sclerosis: an important role for post-translational modifications of myelin basic protein in pathogenesis. Mol Cell Proteomics, 2003. 2(7): p. 453–62. [PubMed: 12832457]
10. Hains PG and Truscott RJW, Age-Dependent Deamidation of Lifelong Proteins in the Human Lens. Investigative Ophthalmology & Visual Science, 2010. 51(6): p. 3107–3114. [PubMed: 20053973]
11. Hooi MYS, Raftery MJ, and Truscott RJW, Racemization of Two Proteins over Our Lifespan: Deamidation of Asparagine 76 in γS Crystallin Is Greater in Cataract than in Normal Lenses across the Age RangeRacemization and Cataract Formation. Investigative Ophthalmology & Visual Science, 2012. 53(7): p. 3554–3561. [PubMed: 22531704]
12. Friedrich MG, et al. , Isoaspartic acid is present at specific sites in myelin basic protein from multiple sclerosis patients: could this represent a trigger for disease onset? Acta Neuropathologica Communications, 2016. 4(1): p. 1–12. [PubMed: 26727948]
13. Hooi M and Truscott R, Racemisation and human cataract. d-Ser, d-Asp/Asn and d-Thr are higher in the lifelong proteins of cataract lenses than in age-matched normal lenses. AGE, 2011. 33(2): p. 131–141. [PubMed: 20686926]

14. Baldensperger T, et al. , Comprehensive analysis of posttranslational protein modifications in aging of subcellular compartments. Scientific Reports, 2020. 10(1): p. 7596. [PubMed: 32371922]
15. Schey KL, et al. , Spatiotemporal changes in the human lens proteome: Critical insights into long-lived proteins. Progress in Retinal and Eye Research, 2019: p. 100802. [PubMed: 31704338]
16. Truscott RJW and Friedrich MG, Molecular Processes Implicated in Human Age-Related Nuclear Cataract. Investigative Ophthalmology & Visual Science, 2019. 60(15): p. 5007–5021. [PubMed: 31791064]
17. Zhu X, Korlimbinis A, and Truscott RJ, Age-dependent denaturation of enzymes in the human lens: a paradigm for organismic aging? Rejuvenation Res, 2010. 13(5): p. 553–60. [PubMed: 20586645]
18. Dovrat A, Scharf J, and Gershon D, Glyceraldehyde 3-phosphate dehydrogenase activity in rat and human lenses and the fate of enzyme molecules in the aging lens. Mechanisms of Ageing and Development, 1984. 28(2): p. 187–191. [PubMed: 6521503]
19. Augusteyn RC, On the growth and internal structure of the human lens. Experimental eye research, 2010. 90(6): p. 643–654. [PubMed: 20171212]
20. Lynnerup N, et al. , Radiocarbon Dating of the Human Eye Lens Crystallines Reveal Proteins without Carbon Turnover throughout Life. PLoS ONE, 2008. 3(1): p. e1529. [PubMed: 18231610]
21. Linetsky M, et al. , Dehydroalanine crosslinks in human lens. Exp Eye Res, 2004. 79(4): p. 499–512. [PubMed: 15381034]
22. Wang Z, et al. , Human protein aging: modification and crosslinking through dehydroalanine and dehydrobutyrine intermediates. Aging Cell, 2014. 13(2): p. 226–34. [PubMed: 24134651]
23. Friedrich MG, et al. , Spontaneous cross-linking of proteins at aspartate and asparagine residues is mediated via a succinimide intermediate. Biochem J, 2018. 475(20): p. 3189–3200. [PubMed: 30181147]
24. Lyons B, Kwan AH, and Truscott RJ, Spontaneous cleavage of proteins at serine and threonine is facilitated by zinc. Aging Cell, 2016. 15(2): p. 237–44. [PubMed: 26751411]
25. Radzicka A and Wolfenden R, Rates of Uncatalyzed Peptide Bond Hydrolysis in Neutral Solution and the Transition State Affinities of Proteases. Journal of the American Chemical Society, 1996. 118(26): p. 6105–6109.
26. Voorter CE, et al. , Spontaneous peptide bond cleavage in aging alpha-crystallin through a succinimide intermediate. J Biol Chem, 1988. 263(35): p. 19020–3. [PubMed: 3198609]
27. Sadeh T and Patchornik A, Nonenzymatic Cleavages of Peptide Chains at the Cysteine and Serine Residues through Their Conversion to Dehydroalanine (DHAL). II. The Specific Chemical Cleavage of Cysteinyl Peptides. Journal of the American Chemical Society, 1964. 86(6): p. 1212–1217.
28. Inglis AS, Cleavage at aspartic acid. Methods Enzymol, 1983. 91: p. 324–32. [PubMed: 6304451]
29. Joshi AB, et al. , Studies on the Mechanism of Aspartic Acid Cleavage and Glutamine Deamidation in the Acidic Degradation of Glucagon. Journal of Pharmaceutical Sciences, 2005. 94(9): p. 1912–1927. [PubMed: 16052557]
30. Friedrich MG, et al. , Mechanism of protein cleavage at asparagine leading to protein–protein cross-links. Biochemical Journal, 2019. 476(24): p. 3817–3834. [PubMed: 31794011]
31. Wang Z, et al. , Cleavage C-terminal to Asp leads to covalent crosslinking of long-lived human proteins. Biochimica et Biophysica Acta (BBA) - Proteins and Proteomics, 2019. 1867(9): p. 831–839. [PubMed: 31226490]
32. Koretz JF, Cook CA, and Kuszak JR, The zones of discontinuity in the human lens: development and distribution with age. Vision Res, 1994. 34(22): p. 2955–62. [PubMed: 7975329]
33. Wang Z and Schey KL, Quantification of thioether-linked glutathione modifications in human lens proteins. Exp Eye Res, 2018. 175: p. 83–89. [PubMed: 29879394]
34. Wessel D and Flügge UI, A method for the quantitative recovery of protein in dilute solution in the presence of detergents and lipids. Analytical Biochemistry, 1984. 138(1): p. 141–143. [PubMed: 6731838]
35. Cox J, et al. , Accurate proteome-wide label-free quantification by delayed normalization and maximal peptide ratio extraction, termed MaxLFQ. Mol Cell Proteomics, 2014. 13(9): p. 2513–26. [PubMed: 24942700]

36. Wang Z, et al. , Proteomics and phosphoproteomics analysis of human lens fiber cell membranes. Invest Ophthalmol Vis Sci, 2013. 54(2): p. 1135–43. [PubMed: 23349431]

37. Lyons B, Kwan AH, and Truscott RJW, Spontaneous cleavage of proteins at serine and threonine is facilitated by zinc. Aging cell, 2016. 15(2): p. 237–244. [PubMed: 26751411]

38. Geiger T and Clarke S, Deamidation, isomerization, and racemization at asparaginyl and aspartyl residues in peptides. Succinimide-linked reactions that contribute to protein degradation. J Biol Chem, 1987. 262(2): p. 785–94. [PubMed: 3805008]

39. Capasso S, et al. , First evidence of spontaneous deamidation of glutamine residue via cyclic imide to α- and γ-glutamic residue under physiological conditions. Journal of the Chemical Society, Chemical Communications, 1991(23): p. 1667–1668.

40. Riggs DL, et al. , Analysis of Glutamine Deamidation: Products, Pathways, and Kinetics. Analytical Chemistry, 2019. 91(20): p. 13032–13038. [PubMed: 31498611]

41. Nalbone JM, et al. , Glutamic Acid Selective Chemical Cleavage of Peptide Bonds. Organic Letters, 2016. 18(5): p. 1186–1189. [PubMed: 26866465]

42. Korlimbinis A, et al. , Protein aging: Truncation of aquaporin 0 in human lens regions is a continuous age-dependent process. Experimental Eye Research, 2009. 88(5): p. 966–973. [PubMed: 19135052]

43. Friedrich MG, et al. , Spontaneous protein–protein crosslinking at glutamine and glutamic acid residues in long-lived proteins. Biochemical Journal, 2021. 478(2): p. 327–339. [PubMed: 33345277]

44. Lieberman AP, Shakkottai VG, and Albin RL, Polyglutamine Repeats in Neurodegenerative Diseases. Annual Review of Pathology: Mechanisms of Disease, 2019. 14(1): p. 1–27.

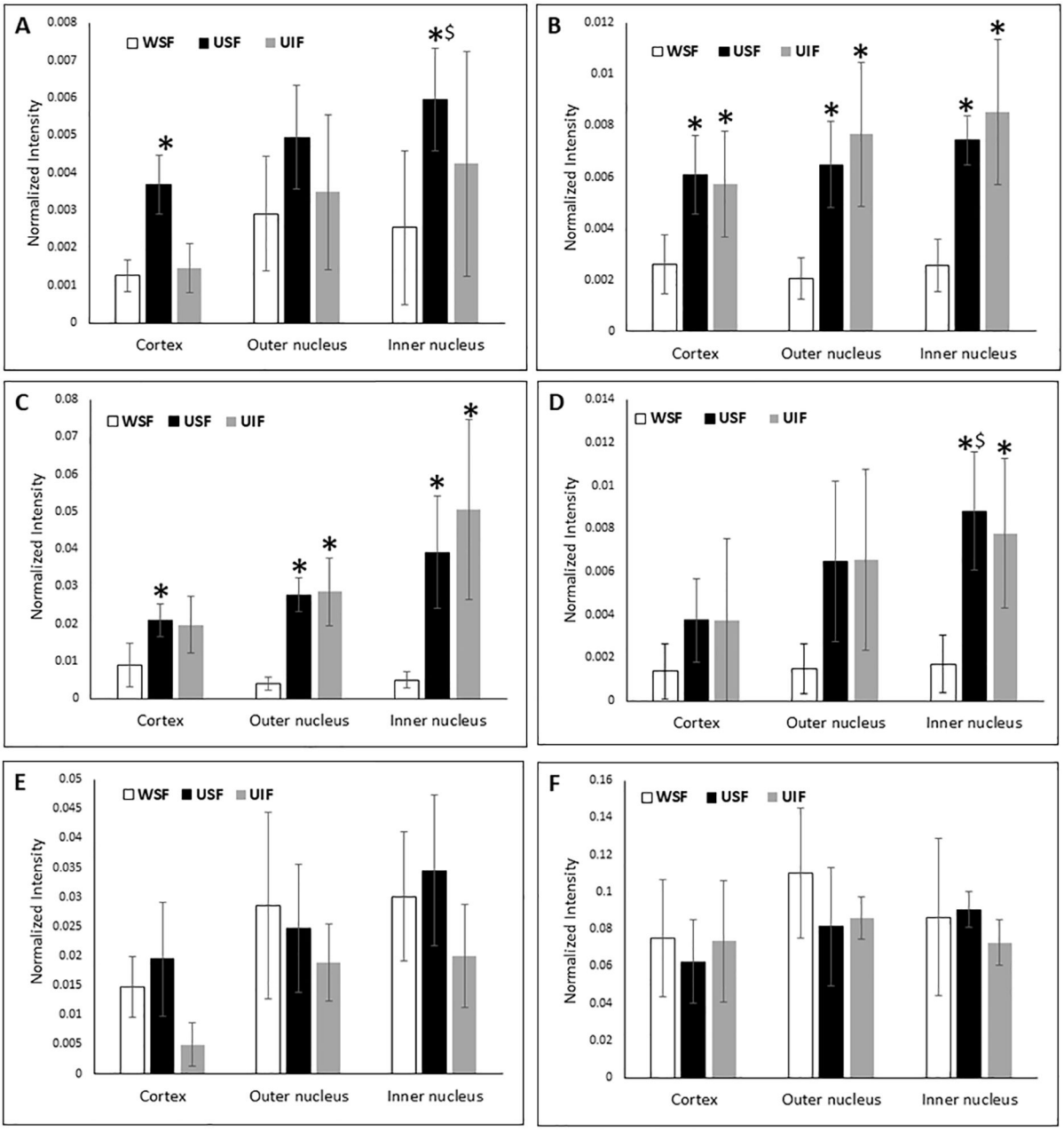

Figure 1: Relative quantification of truncation at Gln and Glu in middle-aged normal human lenses.

Relative truncation of αA E165 (A), αA E156 (B), βA3 Q208 (C), βA4 Q189 (D), βB1 E249 (E) and βB2 Q197 (F) in different regions of middle-aged normal human lenses. * indicates a statistically significant difference in truncation compared with WSF of the same regions of the lens ($p < 0.05$). $ indicates a statistically significant difference in truncation compared with cortex region of the lens. The error bars indicate standard deviation of four biological replicates (WSF = Water soluble fraction, USF = Urea soluble fraction and UIF=Urea insoluble fraction.)

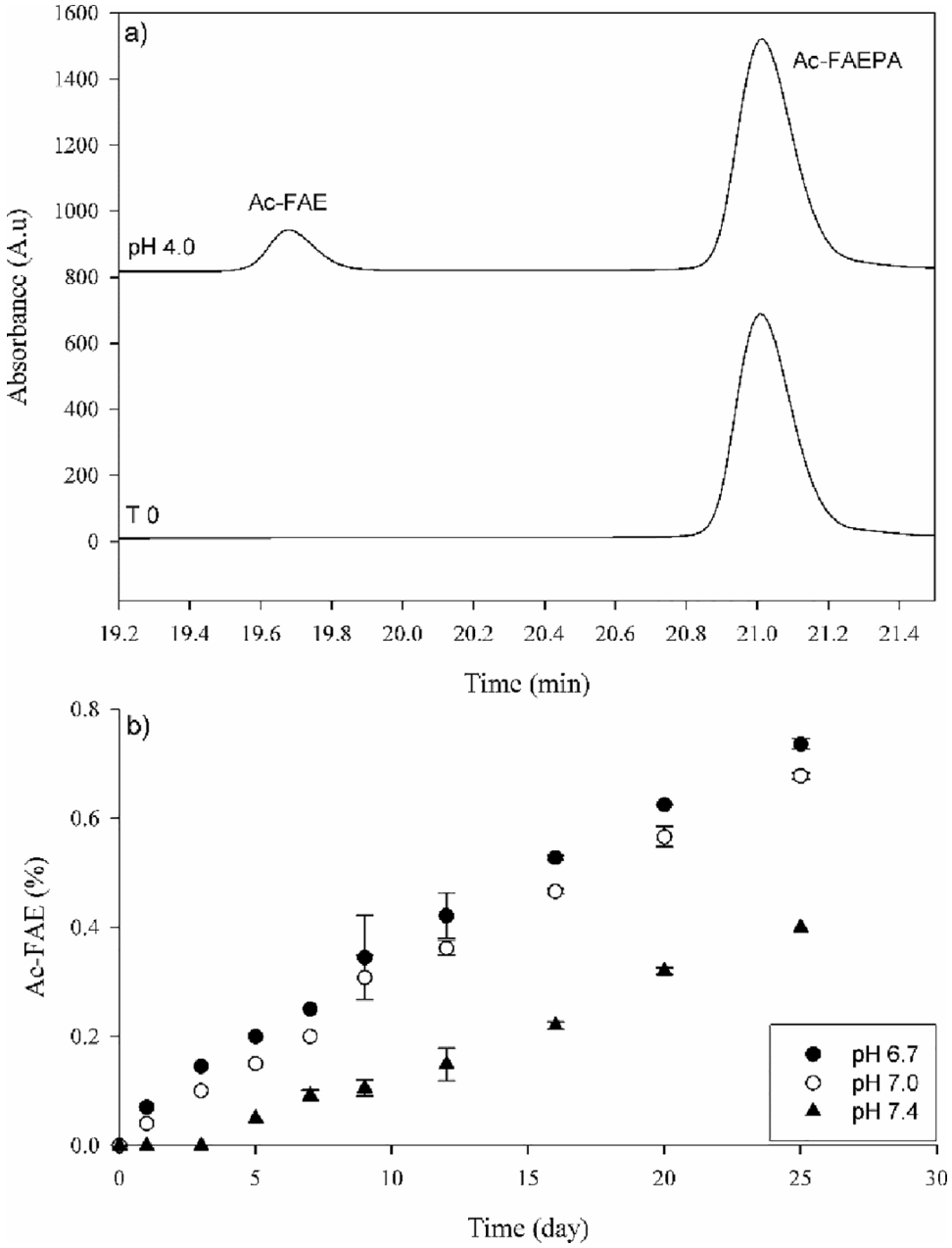

Figure 2. Cleavage on the C-terminal side of Glu in Ac-FAEPA.

a) HPLC profile of Ac-FAEPA at time zero (bottom) and after incubation for 25 days at 60°C, pH 4.0 (Top). The identification of Ac-FAE was confirmed by mass spectrometry. b) Time course of Ac-FAE formation at pH 6.7, 7.0 and 7.4. Ac-FAE was calculated as a percentage of total HPLC peak area. All samples were run in triplicate. Error bars +/− SD.

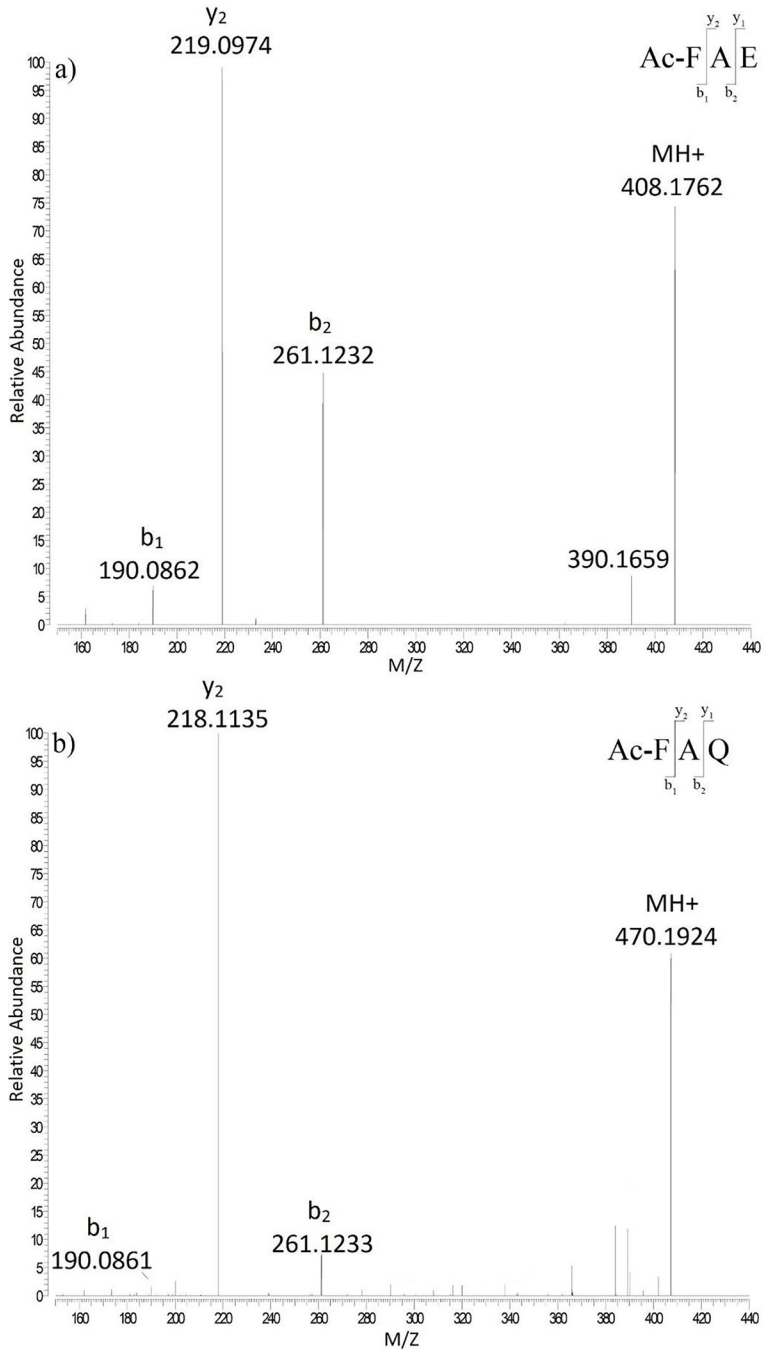

Figure 3. MS/MS spectrum of Ac-FAE and Ac-FAQ isolated from the Ac-FAEPA and Ac-FAQPA incubation.

a) Ac-FAE b) Ac-FAQ following incubation at pH 6.7.

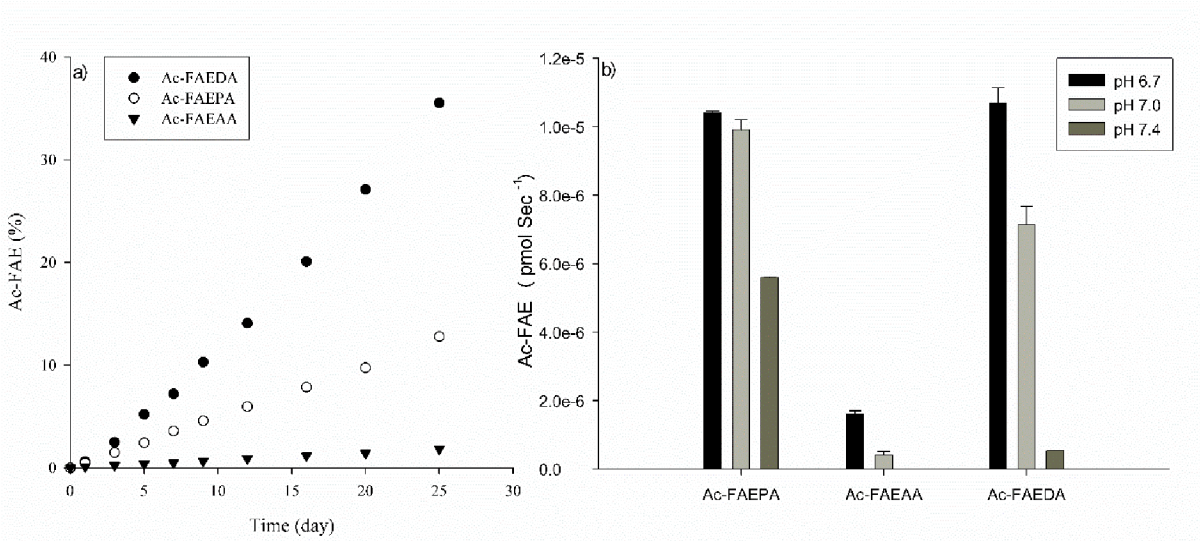

Figure 4. Cleavage on the C-terminal side of Glu in Ac-FAEDA, Ac-FAEPA and Ac-FAEAA.

a) Time course of Ac-FAE from the three peptides at pH 4.0. Ac-FAE formation was calculated as a percentage of total HPLC peak area b) Apparent rate of Glu cleavage in Ac-FAEDA Ac-FAEPA and Ac-FAEAA incubated at pH 6.7, 7.0 and 7.4. Cleavage rate was determined by the slope of the curve over a 25 day incubation period. All samples were run in triplicate at 60°C. Error bars +/− SD.

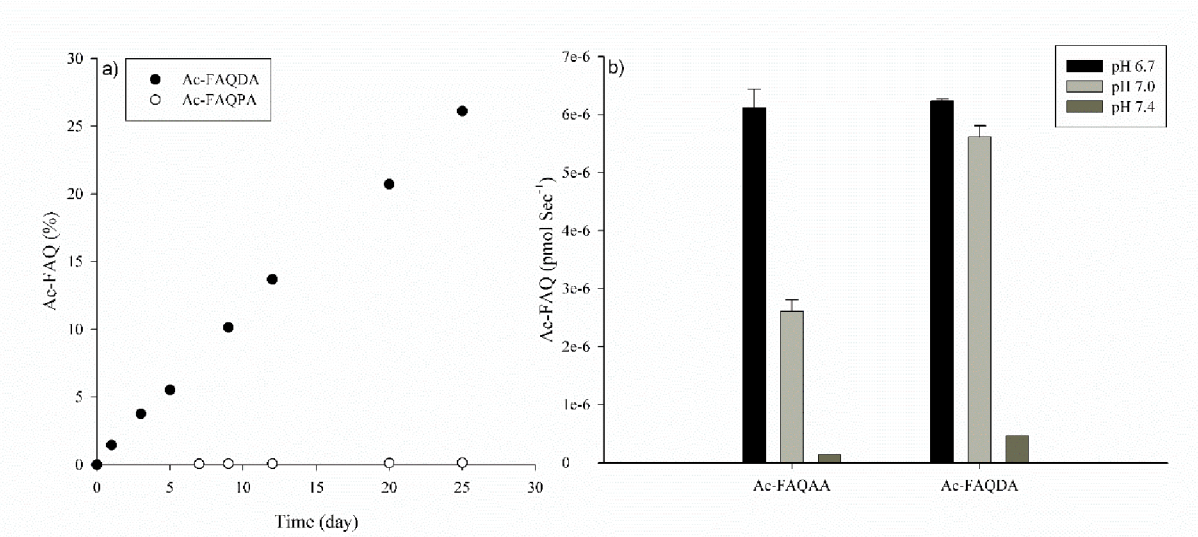

Figure 5. Cleavage on the C-terminal side of Gln in Ac-FAQDA, Ac-FAQPA and Ac-FAQAA

a) Time course of formation of Ac-FAQ from Ac-FAQDA and Ac-FAQPA following incubation at pH 4.0, 60°C. No cleavage of Ac-FAQAA was observed at pH 4.0. b) Apparent rate of formation of Ac-FAQ from Ac-FAQDA and Ac-FAQAA incubated at pH 6.7, 7.0 and 7.4. No cleavage of Ac-FAQPA was observed at these pHs. Cleavage rate was determined by the slope of the line over 25 days at 60°C. All samples were run in triplicate. Error bars +/− SD.

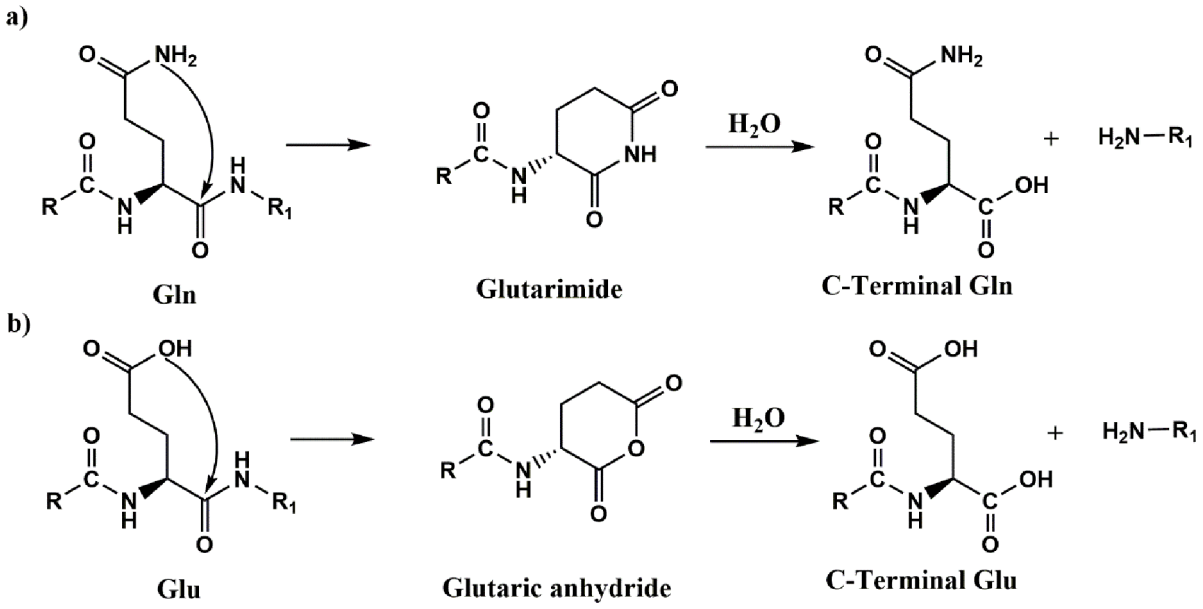

Figure 6. Proposed mechanism of spontaneous cleavage at Gln and Glu in polypeptides.

a) The side chain nitrogen atom of Gln attacks the peptide carbonyl on the C-terminal side of Gln. A glutarimide is formed which is accompanied by cleavage of the peptide bond leading ultimately, after hydrolysis, to the formation of a C-terminal Gln. b) The side chain oxygen atom of Glu attacks the peptide carbonyl on the C-terminal side of Gln. A glutaric anhydride is formed accompanied by cleavage of the peptide bond ultimately leading to the formation of a C-terminal Glu residue.

Table 1:

Sites of cleavage at Gln

Gene Name	Peptide	Cleavage Site	$[MH]^+_{Exp}$	$[MH]^+_{Cal}$
CRYAA	79–90: HFSPEDLTVKVQ	Q90	1399.7216	1399.7212
CRYAA	89–104: VQDDFVEIHGKH**N**ERQ	Q104	1951.9255	1951.9257
CRYAA	120–126: LPS**N**VDQ	Q126	773.3674	773.3676
CRYAB	93–108: VLGDVIEVHGKHEERQ	Q108	1844.9613	1844.9613
HSPG2	486–501: GMVFGIPDGVLELVPQ	Q501	1670.8816	1670.8822
CRYBA1	197–206: EWGSHAQTSQ	Q206	1130.4863	1130.4861
CRYBA1	197–208: EWGSHAQTSQIQ	Q208	1371.6288	1371.6287
CRYBA4	49–63: VLSGAWVGFEHAGFQ	Q63	1604.7854	1604.7856
CRYBA4	178–189: EWGSHAPTFQVQ	Q189	1386.6437	1386.6437
CRYBB1	61–70: LVVFELENFQ	Q70	1237.6480	1237.6463
CRYBB1	93–106: SIIVSAGPWVAFEQ	Q106	1503.7843	1503.7842
CRYBB1	136–147: LMSFRPIKMDAQ	Q147	1436.7382	1436.7390
CRYBB1	151–167: ISLFEGANFKGNTIEIQ	Q167	1882.9435	1882.9433
CRYBB1	215–223: HW**N**EWGAFQ	Q223	1175.4905	1175.4905
CRYBB1	215–225: HWNEWGAFQPQ	Q225	1399.6178	1399.6178
CRYBB1	215–227: HWNEWGAFQPQ**M**Q	Q227	1674.7118	1674.7118
CRYBB2	49–55: AGSVLVQ	Q55	673.3879	673.3879
CRYBB2	172–185: DSSDFGAPHPQVQ	Q185	1384.6125	1384.6128
CRYBB2	190–197: IRDMQWHQ	Q197	1113.5258	1113.5258
BASP1	98–106: AEPPKAPEQ	Q106	966.4891	966.4891
BASP1	98–108: AEPPKAPEQEQ	Q108	1223.5901	1223.5902
BASP1	150–160: KTEAPAAPAAQ	Q160	1054.5528	1054.5527
BFSP1	223–238: SQLEEGREVLSHLQAQ	Q238	1823.9251	1823.9246
BFSP1	320–334: LTSAFIETPIPLFTQ	Q334	1677.9099	1677.9098
ALDOA	260–275: TVPPAVTGITFLSGGQ	Q275	1544.8314	1544.8319
CRYGC	60–67: RGEYPDYQ	Q67	1027.4480	1027.4479
CRYGC	60–68: RGEYPDYQQ	Q68	1155.5062	1155.5065
CRYGC	143–149: QYLLRPQ	Q149	917.5202	917.5203
CRYGD	60–67: RGDYADHQ	Q67	961.4121	961.4122
CRYGS	85–93: AVHLPSGGQ	Q93	865.4529	865.4526
CRYGS	132–149: VLEGVWIFYELP**N**YRGRQ	Q149	2240.1481	2240.1503
CRYGS	159–171: KPIDWGAASPAVQ	Q171	1339.7005	1339.7005
GJA3	108–114: EREEEEQ	Q114	948.3907	948.3905
GJA8	110–116: EAEELGQ	Q116	775.3468	775.3468
GJA8	110–117: EAEELGQQ	Q117	903.4054	903.4054
MIP	239–248: GAKPDVS**N**GQ	Q248	973.4585	973.4585

Gene Name	Peptide	Cleavage Site	$[MH]^+_{Exp}$	$[MH]^+_{Cal}$
MIP	239–261: GAKPDVS**N**GQPEVTGEPVEL**N**TQ	Q261	2368.1150	2368.1151
BFSP2	77–86: ALGISSVFLQ	Q86	1034.5882	1034.5881

Bold and underlined N represents deamidated Asn, Bold and underlined M represents oxidized Met. $[MH]^+_{Exp}$ reports measured masses after recalibration by MaxQuant.

Table 2:

Sites of cleavage at Glu

Gene Name	Peptide	Cleavage Site	$[MH]^+_{Exp}$	$[MH]^+_{Cal}$
CRYAA	22–33: LFDQFFGEGLFE	E33	1448.6733	1448.6733
CRYAA	71–83: FVIFLDVKHFSPE	E83	1577.8361	1577.8362
CRYAA	146–156: IQTGLDATHAE	E156	1155.5641	1155.5640
CRYAA	158–164: AIPVSRE	E164	771.4359	771.4359
CRYAA	158–165: AIPVSREE	E165	900.4785	900.4785
CRYAB	23–30: LFDQFFGE	E30	1002.4565	1002.4567
CRYAB	23–34: LFDQFFGEHLLE	E34	1494.7264	1494.7264
CRYAB	93–106: VLGDVIEVHGKHEE	E106	1560.8083	1560.8016
CRYAB	150–156: KQVSGPE	E156	744.3887	744.3886
CRYAB	158–164: TIPITRE	E164	829.4778	829.4778
CRYAB	158–165: TIPITREE	E165	958.5204	958.5204
CRYBA1	96–108: WDAWSGSNAYHIE	E108	1536.6388	1536.6390
CRYBA4	26–32: RHEFTAE	E32	889.4163	889.4163
CRYBB1	61–67: LVVFELE	E67	848.4765	848.4764
CRYBB1	73–79: RAEFSGE	E79	795.3631	795.3632
CRYBB1	93–105: SIIVSAGPWVAFE	E105	1375.7262	1375.7263
CRYBB1	232–240: LRDKQWHLE	E240	1224.6484	1224.6484
CRYBB1	236–249: QWHLEGSFPVLATE	E249	1613.7958	1613.7958
CRYBB2	161–167: GLQYLLE	E167	835.4559	835.4560
BPGM	63–82: SIHTAWLILEELGQEWVPVE	E82	2349.2125	2349.2125
BASP1	26–33: AEGAATEE	E33	777.3267	777.3261
BASP1	26–34: AEGAATEEE	E34	906.3687	906.3687
BASP1	26–39: AEGAATEEEGTPKE	E39	1418.6281	1418.6281
BASP1	39–53: ESEPQAAAEPAEAKE	E53	1556.7078	1556.7075
BASP1	98–105: AEPPKAPE	E105	838.4296	838.4305
BASP1	98–107: AEPPKAPEQE	E107	1095.5316	1095.5317
BASP1	122–131: AAEAAAAPAE	E131	871.4155	871.4156
BASP1	150–161: KTEAPAAPAAQE	E161	1183.5949	1183.5953
DBN1	187–194: EEELRKEE	E194	1061.5110	1061.5110
DBN1	187–195: EEELRKEEE	E195	1190.5535	1190.5535
BFSP1	312–326: IIEIEGNRLTSAFIE	E326	1704.9167	1704.9167
BFSP1	454–463: SPKEPETPTE	E463	1114.5264	1114.5263
CRYGS	37–43: CNSIKVE	E43	849.4130	849.4135
GJA3	110–118: EEEEQLKRE	E118	1189.5695	1189.5695
GJA8	234–241: SALKRPVE	E241	899.5309	899.5309
GJA8	238–249: RPVEQPLGEIPE	E249	1363.7215	1363.7216

Gene Name	Peptide	Cleavage Site	$[MH]^+_{Exp}$	$[MH]^+_{Cal}$
GJA8	274–283: IVSHYFPLTE	E283	1205.6200	1205.6201
GJA8	274–288: IVSHYFPLTEVGMVE	E288	1720.8613	1720.8615
PYGB	725–731: KGYNARE	E731	837.4220	837.4213
LCTL	451–464: GYTSWSLLDKFEWE	E464	1760.8176	1760.8166
MIP	239–250: GAKPDVS**N**GQPE	E250	1199.5539	1199.5539
MIP	239–254: GAKPDVS**N**GQPEVTGE	E254	1585.7340	1585.7340
MIP	239–257: GAKPDVS**N**GQPEVTGEPVE	E257	1910.8978	1910.8980
NDUFA13	69–78: IALLPLLQAE	E78	1080.6664	1080.6663
BFSP2	90–102: SSGLATVPAPGLE	E102	1198.6306	1198.6314
BFSP2	90–109: SSGLATVPAPGLERDHGAVE	E109	1962.9881	1962.9879
BFSP2	282–289: DVEKNRVE	E289	989.4897	989.4898
BFSP2	401–413: DVASYHALLDREE	E413	1517.7230	1517.7231
EPB41	451–460: IRPGEQEQYE	E460	1248.5855	1248.5855
SPTAN1	64–70: LQIASDE	E70	775.3832	775.3832
WFS1	27–34: LNATASLE	E34	819.4098	819.4094

Bold and underlined **N** represents deamidated Asn. $[MH]^+_{Exp}$ reports measured masses after recalibration by MaxQuant.